Hindawi
Advances in Civil Engineering
Volume 2019, Article ID 9687843, 12 pages
https://doi.org/10.1155/2019/9687843

Research Article

Experimental Study of the Pore Structure Deterioration of Sandstones under Freeze-Thaw Cycles and Chemical Erosion

Jielin Li,[1,2,3] **Rennie B. Kaunda**,[2] **Longyin Zhu**,[1,3] **Keping Zhou**,[1,3] **and Feng Gao**[1,3]

[1]*School of Resources and Safety Engineering, Central South University, Changsha, Hunan 410083, China*
[2]*Department of Mining Engineering, Colorado School of Mines, 1600 Illinois Street, Golden, Colorado 80401, USA*
[3]*Research Center for Mining Engineering and Technology in Cold Regions, Central South University, Changsha 410083, China*

Correspondence should be addressed to Jielin Li; lijielin@163.com

Received 4 August 2018; Revised 23 October 2018; Accepted 16 December 2018; Published 16 January 2019

Academic Editor: Yinshan Tang

Copyright © 2019 Jielin Li et al. This is an open access article distributed under the Creative Commons Attribution License, which permits unrestricted use, distribution, and reproduction in any medium, provided the original work is properly cited.

The issue of rock deterioration in chemical environments has drawn much attention in recent years in the rock engineering community. In this study, a series of 30 freeze-thaw cycling tests are conducted on sandstone samples soaked in H_2SO_4 solution and in pure water, prior to the application of nuclear magnetic resonance (NMR) on the rock specimens. The porosity of the sandstone, the distribution of transverse relaxation time T_2, and the NMR images are acquired after each freeze-thaw cycle. The pore size distribution curves of the sandstone after freeze-thaw cycles, four categories of pore scale, and the features of freeze-thaw deterioration for pores of different sizes in H_2SO_4 solution and pure water are established. The result shows that, with the influence of the acid environment and the freeze-thaw cycles, the mass of the samples largely deteriorates. As the freeze-thaw cycles increase, the porosity of rocks increases approximately linearly. The distribution of the NMR T_2 develops gradually from 4 peaks to 5 or even to 6. Magnetic resonance imaging (MRI) dynamically displays the process of the freeze-thaw deterioration of the microstructure inside the sandstones under acid conditions. The results also show pore expansion in rocks under the coupling effects of chemistry and the freeze-thaw cycles, which differ largely from the freeze-thaw deterioration of the rock specimens placed in pure water.

1. Introduction

The issue of rock deterioration in chemical environments has drawn much attention in recent years in the rock engineering community due to hazards and risks posed to engineered structures. Corrosion due to hydrochemical solutions can cause changes in mineralogical composition and structure of rocks leading to the transformation of the physical mechanical properties of rocks. Therefore, the hydrochemically altered state of rock can pose a great threat to the long-term stability of rock engineering structures [1, 2]. The chemical elements in solution can drive the expansion of cracks and the rate of the crack expansion. In addition, the stress strength factor and the stress strength coefficient of quartz materials are influenced by deionized water, HCl, NaOH, and other acids and bases [3].

The chemical atmospheres may cause damage to all types of stones, especially calcite stones, and the effect of acid atmospheres is related with porosity [4]. In the chemical environment, the mineral components in rocks tend to react with solutions, via complex processes and mechanisms. Previous studies have been carried out to investigate the characteristics of chemical deterioration of rocks; for instance, Feucht and Logan [5] evaluated the effect of chemical solutions (NaCl, $CaCl_2$, and Na_2SO_4 solutions) on the frictional properties of quartz-rich sandstones with triaxial compression tests which were made with varying ionic strengths and pH values. Feng et al. [6–8] conducted a good number of laboratory experiments and theoretical analyses, some advanced instruments were used to study the microstructural damage of rocks in the chemical environment, such as CT, SEM, and X-ray analysis, and the research ideas for studying the fracture criteria of fractured rock considering the effect of chemical solution were provided. Other scholars also conducted investigations on the rock damage constitutive model under the effect of chemical corrosion

[9–11]. The results from these previous achievements have provided references for studies of the long-term stability of rock engineering in chemical environments.

As the research continues to advance, the issues of rock deterioration under the multifactor coupling conditions of pressure, chemical, and other factors have drawn increasingly more attention, such as the rock creep behaviour in a chemical environment [12], the damage of physicomechanical parameters of rocks under the coupling effects of chemical environment and stress loading [13, 14], and the mechanical properties of triaxial compression of rocks immersed in different water chemical solutions [15]. However, besides the influence of the complex hydrochemical environment on rock, there is an essential need to study the damaging effect of the freeze-thaw cycles in cold regions on a rock mass [16]. In mines located in cold regions, for example, the freeze-thaw disasters of the rock mass in mines can occur concurrently with the corrosion of the acid waste water, acid rain, or the deicing saline solution used at the mines, whose influences have been known to interact in certain cases [17]. Some research has been performed on the deterioration of the rock mechanics under the decoupling influence of chemistry and the freeze-thaw. Ning et al. [18] conducted the splitting tests of the concrete under the coupling effect of the acid corrosion and the freeze-thaw cycles, studied the features of the surface erosion and the mechanical properties of the concretes that are of different pH values and being processed by different numbers of freeze-thaw cycles, and analyzed the splitting process of the concrete corroded by acid and the freeze-thaw. They found that the acid erosion of concrete is inversely proportional to the pH value, and the erosion begins on the surface of the concrete. The coupling effects of acid erosion and freeze-thaw cycles accelerate the deterioration of mechanical properties of concrete. In the weak acid environment, freeze-thaw cycles play a leading role in concrete erosion. As the pH value decreases, the effect of acid on concrete gradually increases. Shi et al. [19] studied the changes of different chemical diluents in the concrete of Portland in the freeze-thaw environment and adopted SEM to study the mechanism of formation of pores and cracks in the test specimens, and the results show that NaCl, the NaCl-based deicer, and the K-acetate-based deicer were the most deleterious to the concrete. Lu et al. [20] carried out the indoor simulation tests of concretes under the conditions of the dual corrosion of acid-base and freeze-thaw, and he found that both strong acid and alkali are corrosive to concrete. The corrosion of acid, alkali, and freeze-thaw cycle dominates at different times, accelerating the deterioration of mechanical properties concrete. Gao et al. [21] conducted a freeze-thaw cycle experiment on rock samples which were soaked in four different solutions: sulfuric acid solution, sodium hydroxide solution, sodium chloride solution, and pure water, and the microstructural changes of each group of rock samples were tested by nuclear magnetic resonance (NMR). The results have shown that the influences of sodium hydroxide and sodium chloride solutions are the most significant, and the influence of sulfuric acid solution is relatively weak. In the meantime, NMR results show the chemical solutions have great effects on the microstructure of rocks.

In the previous studies, the research objectives are mainly aimed at the physical and mechanical properties of buildings in cold regions under chemical conditions. Therefore, the reported previous studies tend to take concrete as the research objective when studying the mechanical properties of the rocks under the influence of chemistry and freeze-thaw. Given that the focus is on macroscopic fracture features, very few of the studies have evaluated mechanisms related to the structural deterioration of pores; therefore, the results are somewhat limited in terms of mechanisms and characteristics of the deterioration of the rock mass. In this study, with the impact of acid waste water at mines as the engineering background, rock is selected as the research object. The study discusses freeze-thaw cycling tests of sandstone in the acid environment, the acquisition of the mass of the rock specimens, and observed changes, such as the exterior alteration. It also analyzes and discusses the characteristics of the freeze-thaw deterioration of the microstructure of the rocks in the acid environment with nuclear magnetic resonance technique.

2. Materials and Methods

2.1. Materials. The rock specimens consisted of fleshy red, sandstone with a dense-and-fine fragment texture. The specimens were prepared from natural and fresh rocks which had formed at a comparatively deeper level, anisotropic, and without any traces of cracks developed on the joints. According to the results of the X-ray diffraction test, the red sandstone is mainly composed of quartz, albite, aerinite, sanidine, microcline, laumontite, and chabazite. The bulk density of rock was 2.42 g/cm^3. The water absorption test showed that the percent absorption of the rock specimens was 1.65%, the water saturation ratio was 1.74%, and the water saturation coefficient was 0.95. The rocks were prepared as specimens of standard cylinders 50 ± 1 mm in diameter by 30 ± 1 mm tall, according to "The Codes of Rock Tests in Water Conservancy and Hydroelectrical Projects (SL 264-2001)" standards.

2.2. Experimental Setup and Test Procedures. The rock specimens were numbered C1–C9 and F1–F9, respectively, to match with the H_2SO_4 solution group and the pure water group. First, prepare a H_2SO_4 solution with initial pH = 1.5 (the mass concentration of sulfuric acid is 1.5 g/L), according to the lowest pH value in the mine waste water where the sampling site is located. Then, the rock specimens were separately immersed in the H_2SO_4 solution and pure water for 48 hours to reach a state of natural saturation. The volume of the sulfuric acid solution and pure water is based on the thoroughly immersed specimens. It ranges from 2 L to 3 L. Next the rock specimens were placed in a TDS-300 freeze-thaw testing machine for the freeze-thaw cycling tests. According to the requirements of the freeze-thaw test, the parameters of the freeze-thaw were the freezing temperature

was −20°C, the thawing temperature was 20°C, and both the time for freezing and the time for thawing were 4 hours. There were 30 freeze-thaw cycles to undergo, and the rock specimens were numbered 1–3, 4–6, and 7–9 corresponding with 0, 10, 20, and 30 freeze-thaw cycles, respectively. At the end of every 10 freeze-thaw cycles, the rock specimens were extracted to conduct the NMR tests using an AniMR-150 MRI analyzing system (Suzhou Niumag Electronic Technology Co., Ltd.). As shown in Figure 1, in the NMR porosity test, the rock specimens that have completed the freeze-thaw cycle test are taken out from pure water or H_2SO_4 solution, and the surface moisture (or solution) is wiped with a towel, wrapped with a plastic wrap (to prevent evaporation of water), and then placed in the MRI analyzing system.

The AniMR-150 MRI analysis system is mainly composed of the spectrometer system, RF unit, magnet cabinet, industrial personal computer, and inversion software. The device is developed on the basis of a ^1H relaxation response. The main magnetic field of the MRI system is 0.3 ± 0.05 Tesla, the diameter of the probe coil is 150 mm, the main frequency of instrument is 12.8 MHz, the gain of the receiver is greater than 40 dB, and the maximum sampling bandwidth is greater than 300 kHz; the RF power is 300 W, and the maximum resolution of MRI is 100 μm. The number of sampling peaks can reach 18,000, the echo time is less than 150 ms, and the sample relaxation time is measured from 80 μs to 14 s [22].

In the NMR test, the transverse relaxation time (T_2) was retrieved by using the NMR rock-core analyzing software (Version 1.1.0) [23], which could obtain the intensity of nuclear magnetic signals and T_2 spectra and composite them as the transverse relaxation time of the rock specimen. During the test, one specimen was placed at the center of the radio frequency (RF) coil for CPMG pulse sequence experiments. The experimental parameters were as follows: receiver bandwidth SW = 200 kHz; frequency main value SF = 12 MHz; center frequency O1 = 531730.99 Hz; sampling points TD = 331208; waiting time Tw = 3000 ms; number of echo cycles NECH = 6000; TE = 0.276 ms; coil waiting time RFD = 0.06 ms; analog gain RG1 = 20 db; digital gain RG2 = 4; cumulative sampling NS = 32.

After the test, the decay curve between echo signal and sampling time can be obtained by the AniMR-150 MRI analysis system (Figure 2(a)) and the relationship between porosity increment and T_2 relaxation time distribution (Figure 2(b)) can be derived from the decay curve by inversion methods. The shaded area between the curve and horizontal axis is termed as the spectra area and measured porosity. A final porosity of 3.6% can be obtained from the accumulated porosity curve.

3. Macroscopic Observation and Pore Structure Alteration Based on Quantification of Water Imbibition

The appearance of the rock specimens soaked in H_2SO_4 and pure water after the freeze-thaw tests is as shown in Figures 3 and 4, respectively. A comparison of the appearances of the frozen rock specimens shows that, after 30 freeze-thaw cycles, the surface of the sandstone specimens which were placed in the acid environment was seriously eroded, and the particles on the surface peeled off in large quantities. In contrast, the surface of the sandstone specimens placed in pure water did not show significant changes.

In the following experiment, after every round of freeze-thaw cycles (the number is predetermined), the rock specimens were taken out and wiped dry, and then a mass test was conducted. Therefore, the change in the mass of the rock specimens is also a useful indicator of deterioration. The result of the mass of the rock specimens which changed with the number of freeze-thaw cycles in the acid environment is shown in Figure 5. It is clear from Figure 5 that, after 10 freeze-thaw cycles, the average mass of the rock specimens of the H_2SO_4 solution group and the pure water group increases by 0.20% and 0.16%, respectively. The observed changes in the average mass indicate that the 10 freeze-thaw cycles had led to the expansion of minute cracks in the sandstones to various degrees, and that water had entered the pores, which caused the increase of the mass of rock.

After 20 freeze-thaw cycles, the mass of the specimens begins to show a decrease at various degrees. The mass of the specimens of the H_2SO_4 solution group and the pure water group shows a drop of 0.63% and 0.16%, respectively. By observing the appearance of the specimens, one can find free particles in the solution. Therefore, the 20 freeze-thaw cycles cause the surface of the specimens to undergo macroscopic fracture, resulting in the peeling off of the particles from the rock surface, and the mass of those particles is apparently larger than that of the increase of the pore water. In other words, at the midstage of the freeze-thaw deterioration, the acid environment will influence the freeze-thaw deterioration of the rocks at a comparatively larger scale.

After 30 freeze-thaw cycles, the mass of the rock specimens in pure water almost remains nearly unchanged; however, the surface quality of the rock specimens placed in the H_2SO_4 solution continues to worsen. The implication is that, under the acid conditions, the particles peeled off from the surface of the rock specimens at a higher rate, and the number of free particles in the solution had increased significantly. There is a large number of solid sediments in the solution, leading to the deterioration of the overall quality and integrity of the rock specimens.

4. Pore Structure Alterations Characterized by NMR Response

4.1. Porosity. An assessment of porosity could directly reflect the condition of deterioration within the rock specimens. The AniMR-150 MRI analyzing system was used to measure the porosity of the sandstone specimens after every 10 freeze-thaw cycles, and the results are as shown in Table 1.

Table 1 shows that, with the addition of the freeze-thaw cycles, the porosity of the sandstones generally increases, but the scale of increase of the porosity of the sandstones in H_2SO_4 solution is relatively larger than that of the specimens placed in pure water. It is thus clear that, for the same number of freeze-thaw cycles, the minerals (such as quartz,

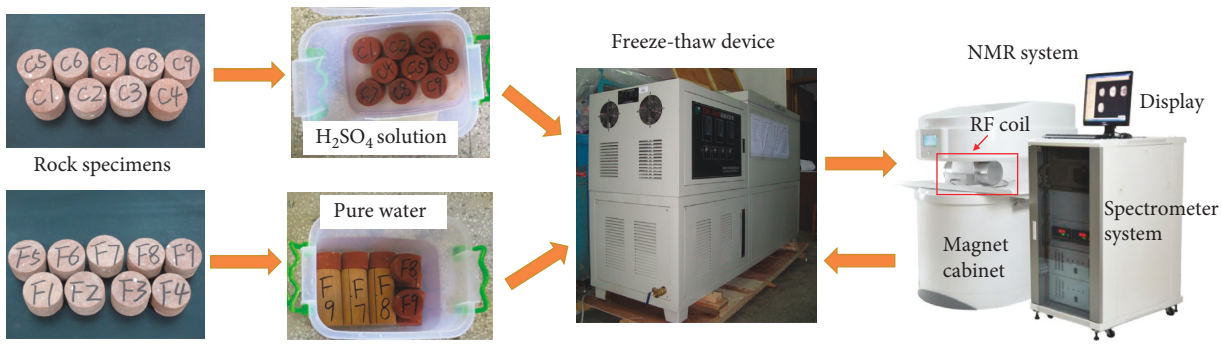

Figure 1: Sequence showing experimental setup and test procedure requiring rock specimen preparation, the TDS-300 freeze-thaw testing machine, and the AniMR-150 MRI analyzing system.

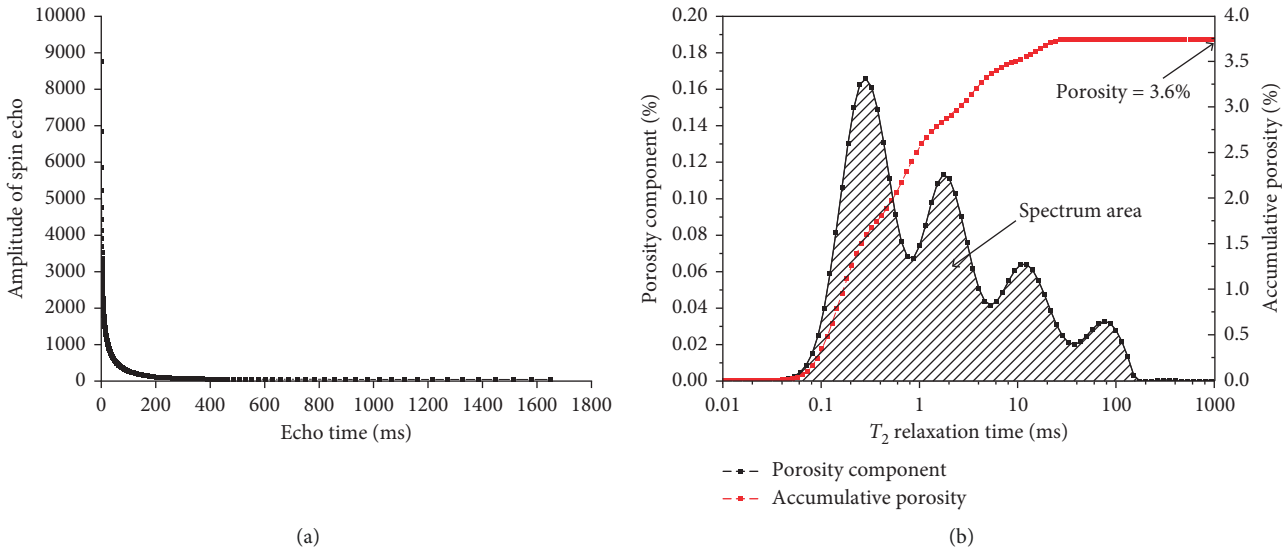

Figure 2: Results of NMR analysis: (a) echo signal decay curve; (b) T_2 relaxation time distribution curve.

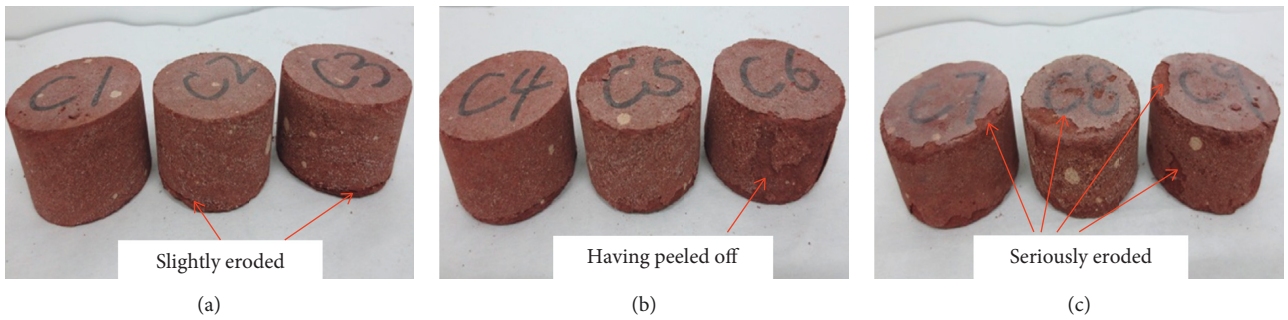

Figure 3: Specimens macroscopic observation after different numbers of freeze-thaw cycles in H_2SO_4 solution: (a) 10 cycles; (b) 20 cycles; (c) 30 cycles.

albite, and microcline) in the sandstones had reacted with H_2SO_4 solution chemically. Therefore, the mineral elements of the rocks changed and the links between particles were weakened, which led to the increase in porosity. This result is in agreement with the changes in the mass and surface appearances of the specimens discussed in Section 3, which shows that the interior and exterior deterioration of rock occurred under the coupling effect of chemistry and the freeze-thaw.

The mean values of the porosity of every group of rock specimens were analyzed and are shown in Table 1. It can be seen that, under the same conditions of freeze-thaw cycling, H_2SO_4 solution apparently accelerated the deteriorating process within the rocks, especially after 10 freeze-thaw

(a) (b) (c)

Figure 4: Specimens macroscopic observation after different numbers of freeze-thaw cycles in pure water: (a) 10 cycles; (b) 20 cycles; (c) 30 cycles.

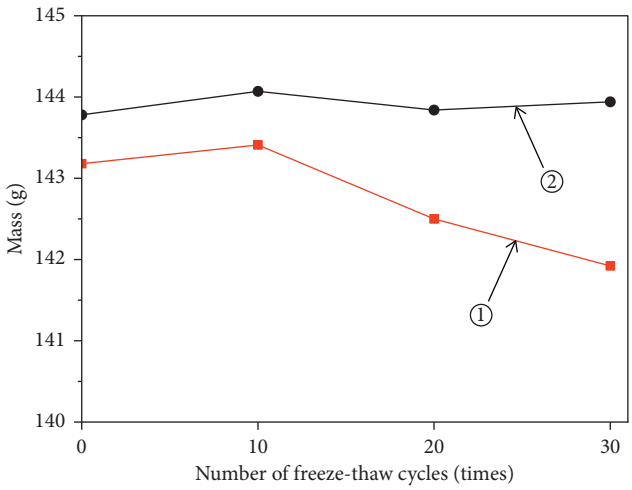

Figure 5: Curve of the changes of the mass of the rock specimens. Two different kinds of solution are labelled by ① H_2SO_4 solution and ② pure water.

Table 1: Result of the measurement of the porosity of the sandstones (porosity (%)).

H_2SO_4 solution					Pure water				
Specimens	Freeze-thaw cycles				Specimens	Freeze-thaw cycles			
	0	10	20	30		0	10	20	30
C7	3.6	4.1	4.5	5.0	F7	3.5	4.0	3.9	4.2
C8	4.0	4.6	5.0	5.4	F8	3.3	3.8	3.7	3.9
C9	3.9	4.3	5.0	5.6	F9	3.2	3.6	3.6	3.8
Average	3.8	4.3	4.8	5.3	Average	3.3	3.8	3.7	4.0

cycles. While the porosity of sandstones in pure water changed little, the mass change is also small. However, the porosity of sandstones in H_2SO_4 solution increased linearly with the increased number of the freeze-thaw cycles. After 30 freeze-thaw cycles, the porosity increased by 39.5% in H_2SO_4 solution and only by 21.2% in pure water. Under the influence of freeze-thaw cycles, the pores inside the rock in pure water continue to develop and expand, and the external moisture enters the newly created or expanded pores, resulting in changes in mass and porosity. In H_2SO_4 solution, freeze-thaw also leads to changes in pores of rock samples. The observed discrepancies in increased porosity indicate that H_2SO_4 solution had entered the newly produced pores of rock and had undergone additional chemical reactions incessantly with some of the activated minerals in the rocks. Therefore, the particles within the rocks corroded continuously, and the mineral elements of the rocks changed. The solutes were drifted out of the rock in water to produce sediments and then resulted in the decrease of mass of the rock specimens (Figure 5). However, the separation of solutes inside the rocks resulted in the formation of cavities, karst voids, and cracks of corrosion. Thus, the acid environment could produce a significant influence on the freeze-thaw deterioration of rock.

4.2. T_2 Spectral Distribution of NMR. Previous studies [24, 25] have shown that the T_2 spectral distribution reflects the size and distribution of the pores of rock specimens. The size of pore is related to the position of the spectral peak; in particular, the group of the small size of pores corresponds to smaller T_2 values, while the group of large size of pores corresponds to larger T_2 values. Figure 6 shows the distribution curves of NMR transverse relaxation time T_2 of the sandstone rock specimens after different numbers of freeze-thaw cycles in H_2SO_4 solution and in pure water. It can be seen that there were mainly four T_2 spectral peaks for the sandstones. With the increase of the number of freeze-thaw cycles and under the influence of freeze-thaw and the acid solution, new pores have developed within the rock, and tiny pores have gradually expanded into large-sized pores. And the number of peaks increased from 4 to 5 or even to 6. It can be seen from Figure 6(b) that, after 30 freeze-thaw cycles, the pores in the rock expand and the large-sized pores increase under the action of freeze-thaw cycles. The water enters the newly created large-sized pores and caused the large pores to "collapse," causing the large-sized pores to be packed and their sizes to be changed. Thus, 30 freeze-thaw cycle samples have shorter T_2 values than after 20 cycles.

Table 2 shows the peak areas of the NMR T_2 spectra of specimens under different conditions. It can be seen from Figure 6 and Table 2 that the individual T_2 spectral distribution of the sandstones in H_2SO_4 solution and in pure water differed largely. After 30 freeze-thaw cycles, the total

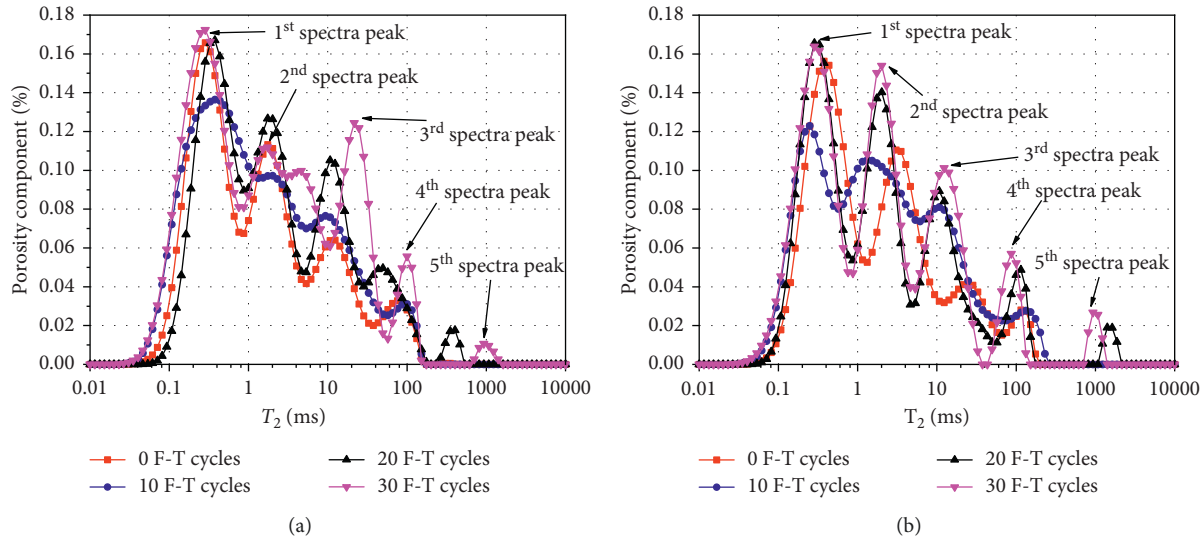

Figure 6: T_2 distribution of sandstones after different numbers of freeze-thaw cycles: (a) H_2SO_4 solution; (b) pure water.

Table 2: Statistics of the proportion of each peak area in the T_2 curve.

Solution	Specimen	Proportion of each peak area (vol.%)						Total peak area
		1st	2nd	3rd	4th	5th	6th	
H_2SO_4	C7-0	48.37	28.27	17.00	6.36	0	0	12467
	C7-10	54.62	19.99	21.46	3.94	0	0	14417
	C7-20	40.12	28.09	20.52	9.89	1.38	0	14378
	C7-30	43.25	18.11	14.93	18.07	4.84	0.80	16903
Pure water	F7-0	51.76	33.24	10.89	4.10	0	0	11614
	F7-10	32.50	40.00	22.46	5.04	0	0	13111
	F7-20	42.87	28.81	20.94	5.82	1.56	0	12835
	F7-30	41.51	29.73	20.44	6.36	1.95	0	14058

spectral area of the rock specimen #C7 (in H_2SO_4 solution) increased by 35.6% and the number of peaks increased from 4 to 6. In the meantime, the total spectral area of the rock specimen #F7 (in pure water) increased by 21%, and the number of peaks increased from 4 to 5.

In addition, the trend of each spectra peak is also different. The proportion of the 4th, 5th, and 6th spectra peaks in H_2SO_4 solution is gradually increasing; that is, the increase of large-sized pores is obvious, especially the 4th spectra peak, which increases by 2.8 times. However, in H_2O solution, it mainly shows that the proportion of the first spectra peak has decreased, and the proportion of the 3rd and 5th spectra peaks has increased. Given that, during the freezing and thawing processes, the moisture within the pores freezes, and the bulk volume expands as a result [26, 27]. Thus, the development and expansion of the pores are accelerated to introduce chemical solution into the new pores. The entry of chemical solution into the new pores would be expected to corrode and lubricate the particles within the rock material. Therefore, the cohesion between the mineral particles decreased, the pores grew larger, and the frictional force was reduced. Under the repeated influence of freezing and thawing, the chemical solution in the pores would be expected to incessantly corrode the minerals in the rock and to destroy the friction and the mineral elements between the mineral particles. Furthermore, the pressure created by the volume expansion after the freezing of moisture would easily reach the extreme tensile strength of the walls of the pores. These changes would lead to a rapid expansion of the tiny pores and cause the larger pores to collapse, which leads to a macroscopic fracturing of the specimens. This chain of events ultimately leads to a macroscopic fracturing, which also explains why the general porosity of rocks increases seemingly linearly.

Table 2 shows that, under the coupling effects of freeze-thaw cycles and chemical conditions, the changing trend of different size pores in rock which has been immersed in pure water and H_2SO_4 solution is different. It also shows that, after the different number of freeze-thaw cycles, the proportion of the second spectrum peak in pure water is significantly higher than the proportion of the second spectrum peak in H_2SO_4. Therefore, the porosity of the component of T_2 spectrum in pure water is higher than that in H_2SO_4, but the total spectrum area is still large in H_2SO_4 solution.

4.3. MRI Results. Figure 7 displays the magnetic resonance imaging (MRI) of the rock specimens after 0, 10, 20, and 30 freeze-thaw cycles in the H_2SO_4 solution. The maximum resolution of the MRI system used in the experiment was

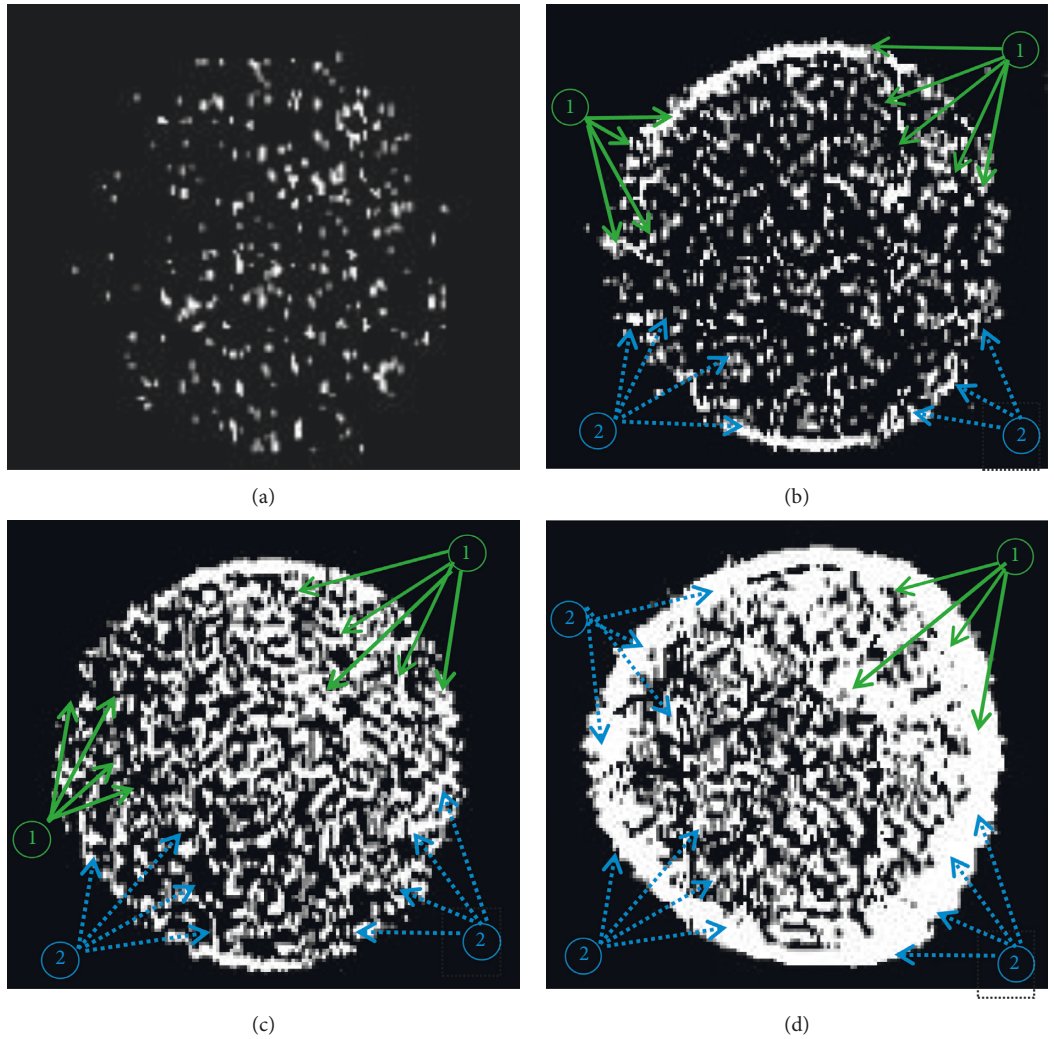

Figure 7: Images of sandstones of the H_2SO_4 solution group after different numbers of freeze-thaw cycles: (a) 0; (b) 10; (c) 20; (d) 30. Two different kinds of pore deformation are approximately labelled by ① which indicates new pores are generated and ② which indicates pores are deformed to larger size.

100 μm, and the image was automatically generated by the NMR test system. The illuminated areas in the image were the places where the moisture was present, and the dark areas represent the background color. The brightness of the image shows the quantity of water content, i.e., the lighter the image, the greater the amount of moisture present in that area, and the larger the pore size in that area. At freeze-thaw cycle at time 0, the light dots in the MRI are well-distributed, which indicates that the interior of the sandstone specimens was perfectly isotropic. After 10 freeze-thaw cycles, the number of light dots increases, which indicates that the number of pores in the rocks had increased. There is a circle of light dots around the contour of the sandstones which had been placed in H_2SO_4 solution, which shows that, with the dual effect of acid corrosion and the freezing and thawing, small cracks on the outer layer of the rock specimens had kept expanding, while the rock specimens in pure water had not shown similar changes (Figure 8(b)).

After 20 freeze-thaw cycles, the number of light dots continue to increase in the MRI of the sandstones in H_2SO_4 solution covering almost the entire section. The size of pores of the rock specimens continues to grow, and the number of large-sized pores continues to grow also, while the pores within the rock specimens in pure water did not display similar changes. After 30 freeze-thaw cycles, the number and size of the light dots in the MRI of the sandstones in H_2SO_4 solution has clearly increased. There is a large quantity of pores on the surface of the rock specimens, and they are surrounded by the pore water. The NMR signals within the rock specimens are very strong, and the areas of light dots are close to connecting with each other. The observed trend shows that the acid solution had affected the interior structure of the sandstone, which had led to the unusual development of the cracks within the rocks and the macroscopic fracture of the appearances of the rock specimens.

In contrast, as shown in Figure 8, the pores inside the rock specimens in pure water do not display significant development and progression, although the results still show the process of the development of pores from the exterior to the interior of the rock specimens under freeze-thaw effects.

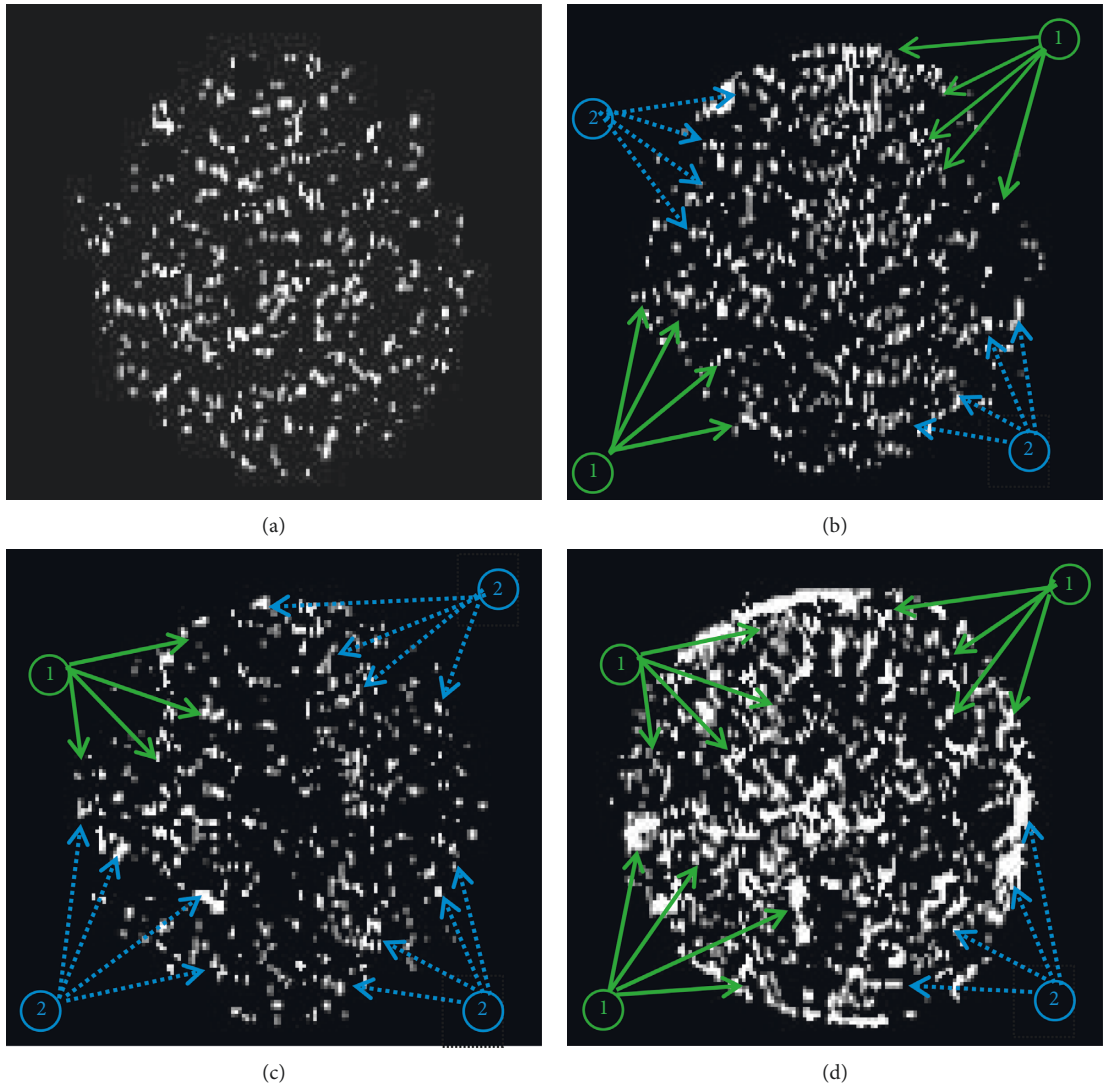

Figure 8: Images of sandstones of the pure water group after different numbers of freeze-thaw cycles: (a) 0; (b) 10; (c) 20; (d) 30. Two different kinds of pore deformation are approximately labelled by ① which indicates new pores are generated and ② which indicates pores are deformed to larger size.

After 30 freeze-thaw cycles, there are some light dots nearly in contact inside and outside the specimens; however, the deterioration remains weak. In addition, close inspection shows that there were relatively few macroscopic cracks formed in the surface appearance of the rock specimens. In summary, the chemical solution had reacted with and corroded the mineral structures in the acidic solution, which caused the inner and outer shapes of rocks and the sizes of particles, pores, and cracks to transform. The chemical etching had largely influenced the development and expansion of the cracks within the sandstone.

5. Discussion

5.1. The Effects of Freeze-Thaw on the Evolution of Rock Pores. The freezing and thawing cycles of the sandstone specimens in both acidic and nonacidic environments affected the size, number, and distribution of pores within the entire rock material, as discussed in Section 4. Consequently, freeze-thaw cycles in such environments have important implications related to the permeability of the sandstones and to the mechanical behaviour of the sandstone. According to the NMR principle, the NMR crosswise relaxation rate $1/T_2$ is given as follows [28, 29]:

$$\frac{1}{T_2} = \rho_2 \left(\frac{S}{V}\right)_{\text{porosity}}, \tag{1}$$

where S is the surface area of a pore (cm^2), V is the pore volume (cm^3), and ρ_2 is the crosswise surface relaxation strength (μm/ms).

If the pore radius is positively related to the throat radius, equation (1) becomes [30, 31]

$$\frac{1}{T_2} = \frac{\rho_2}{r_c} F_s, \tag{2}$$

where r_c is the pore radius and F_s is a geometrical factor (for the spherical pores, $F_s = 3$; and for the columnar pores, $F_s = 2$).

$$r_c = CT_2, \tag{3}$$

where $C = F_s\rho_2$ and C is called the conversion coefficient.

It can be concluded from equations (1)–(3) that the pore radius is in direct proportion to T_2: the smaller the T_2 is, the smaller the represented pore becomes, and the larger the pore, the larger the T_2 becomes.

With the scaling and error analysis of the transverse relaxation time T_2 and pore throat radius, the best scale range of the C value of the red sandstone is between 0.3 and 0.5 μm/ms, and the average value is 0.3125 μm/ms [32]. Therefore, equation (4) can be achieved by simplifying equation (3) as follows:

$$r_c = 0.3125T_2. \tag{4}$$

According to equation (4), T_2 spectra can be transformed into the pore size distribution curve (Figure 9). There has been no agreed standard about the classification of the pore size of sandstone. Based on the result of the classification of the pore size of sandstone acquired by some scholars [33–35], this paper divides the pore sizes into four categories: micropores (diameter < 0.1 μm), minipores (diameters between 0.1 and 1 μm), mesopores (diameters between 1 and 50 μm), and macropores (diameters ≥50 μm). Figure 9 shows the pore size distribution curve of rock specimens which are soaked in H_2SO_4 solution and in pure water after 0 and 30 freeze-thaw cycles, respectively. With the segmented statistics of the pore size distribution curves, the proportion of the distribution of different-sized pores soaked in two solutions after 0, 10, 20, and 30 freeze-thaw cycles are obtained (Table 3).

After 0 and 30 freeze-thaw cycles, the numbers of minipores and mesopores of sandstone in two solutions are dominant. The rock specimen (rock specimen #C7) in H_2SO_4 solution accounts for 74.4% and 74.3%, respectively, after 0 and 30 freeze-thaw cycles, and the rock specimen (rock specimen #F7) in pure water accounts for 82.2% and 75.2%, respectively, after 0 and 30 freeze-thaw cycles. The results show that there are relatively more minipores and mesopores and less micropores and macropores in the initial sandstones. With the growth of freeze-thaw cycles, the pores develop and expand under the coupling effect of freeze-thaw cycles and chemical reaction, and the pores connect with each other. The pore sizes generally expand, and the micropores develop, and the growth of the number of marcopores is the most clear, leading to the transformation of the pore structure of rock specimens.

After 30 freeze-thaw cycles, differences occur in the changes of the pore structure of sandstone in the H_2SO_4 solution and pure water. Part of the minerals dissolve and are separated out and move out of the rocks in the H_2SO_4 solution given that chemical reactions occur between the H_2SO_4 solution and the mineral granules within the rock specimens. Therefore, cavities are formed in the rocks, causing the pore sizes to develop and expand, and the

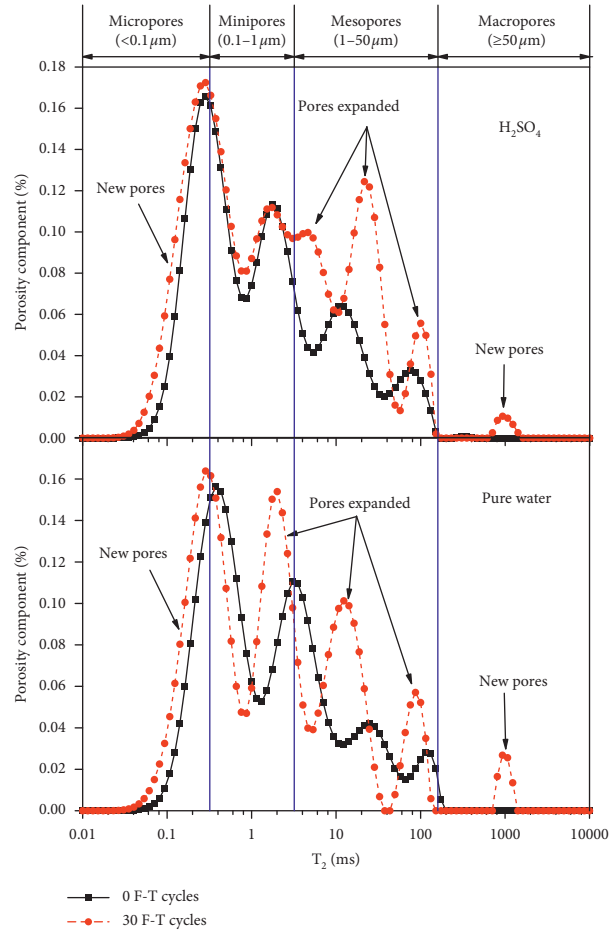

Figure 9: Division of T_2 spectra of sandstone specimens according to pore size in different solutions.

permeability of the rock is improved, which facilitates the movement of the solution and intensifies the chemical reaction. Consequently, the number of mesopores grows by 32.2%, and the number of macropores grows from 0 to 0.8. Conversely, the numbers of micropores and minipores decline, with the decrease ranges of −2.7% and −20.3%, respectively. In contrast, in the pure water where only the influencing factors of frost heave and water movement are significant, the pores develop and expand continuously, which leads to the expansion of pore sizes and the creation of new micropores. Thus, micropores increase by 28.8%, and macropores increase from 0.2 to 2.0; the minipores and mesopores decline, with decreasing ranges of −10.8% and −5.1%, respectively.

5.2. Pore Structure Deterioration under the Coupled Effect of Freeze-Thaw and Chemical Solution. The chemical compositions of red sandstone are shown in Table 4.

It can be seen in Table 4 that the red sandstone is mainly composed of SiO_2, Al_2O_3, CaO, MgO, Na_2O, Fe_2O_3, and other minor chemical elements. Among the constituents, SiO_2 is the major element in the red sandstone. When chemical solutions and rocks were put together during the experiments, a series of complex physical and chemical

Table 3: Proportional variations of pore sizes in different solutions.

Pore size	Proportion of pores in cores in H_2SO_4 solution (%)				Proportion of pores in cores in pure water (%)			
	0 cycle	10 cycles	20 cycles	30 cycles	0 cycle	10 cycles	20 cycles	30 cycles
Micropores (<0.1 μm)	25.5	24.3	15.7	24.8	17.7	20.9	21.1	22.8
Minipores (0.1–1 μm)	45.8	43.4	47.4	36.5	48.9	41.6	47.1	43.6
Mesopores (1–50 μm)	28.6	32.3	35.6	37.8	33.3	36.4	30.3	31.6
Macropores (≥50 μm)	0.0	0.0	1.4	0.8	0.2	1.2	1.6	2.0

Table 4: Chemical composition of red sandstone (%).

SiO_2	Al_2O_3	CaO	MgO	Na_2O	Fe_2O_3	K_2O	TiO_2	P_2O_5
52.5	11.4	5.8	3.8	3.2	2.3	1.8	0.5	0.1

reactions were bound to occur, involving complex processes and mechanisms [36]. Based on the ability of acid-dissolving sandstone minerals, the minerals could be divided into two classes [37]: fast reacting minerals (with strong acid-dissolving ability), which includes aluminosilicate (authigenic clay, feldspar, and calcite), and slow reacting minerals (clay splinter and quartz). During the acid-rock reaction, the H_2SO_4 solution provides H^+ and H_2O.

Under the condition of a strong acid, SO_4^{2-} in the solution slowly reacted or did not react with the major element SiO_2, which caused the difficult dissolution of quartz minerals, and thus, the quartz minerals were prevented from moving out of the rocks. In the unlikely event that there were a few quartz minerals that were dissolved and generated free SiO_4^{2-}, the silicic acid still existed as a single molecule under the strong acid condition where pH = 1–3, and thus, biopolymers that were weak in water solubility would not be produced. Therefore, in the freeze-thaw process, the mass loss of rock specimens occurred slowly. The reason for the mass loss is that other chemical compositions (such as CaO) had dissolved and migrated out of the rocks, explaining why the mass loss of rock specimens was relatively little.

The chemical formulae of chemical reactions between elements such as H^+ and SO_4^{2-} in the H_2SO_4 solution, pure water, Al_2O_3, CaO, and MgO are as follows:

In pure water:

$$CaO + H_2O \longrightarrow Ca(OH)_2 \quad (5)$$

$$Na_2O + H_2O \longrightarrow 2Na(OH) \quad (6)$$

$$K_2O + H_2O \longrightarrow 2K(OH) \quad (7)$$

$$P_2O_5 + H_2O \longrightarrow 2HPO_3 \quad (8)$$

In H_2SO_4:

$$SiO_2 + 2H_2SO_4 \longrightarrow Si(SO_4)_2 + 2H_2O \quad (9)$$

$$Al_2O_3 + 3H_2SO_4 \longrightarrow Al_2(SO_4)_3 + 3H_2O \quad (10)$$

$$CaO + H_2SO_4 \longrightarrow CaSO_4 + H_2O \quad (11)$$

$$MgO + H_2SO_4 \longrightarrow MgSO_4 + H_2O \quad (12)$$

$$Na_2O + H_2SO_4 \longrightarrow Na_2SO_4 + H_2O \quad (13)$$

$$Fe_2O_3 + 3H_2SO_4 \longrightarrow Fe_2(SO_4)_3 + 3H_2O \quad (14)$$

$$K_2O + H_2SO_4 \longrightarrow K_2SO_4 + H_2O \quad (15)$$

$$P_2O_5 + 3H_2SO_4 \longrightarrow 2H_3PO_4 + 3SO_3 \quad (16)$$

According to chemical formula (11), slightly soluble element $CaSO_4$ was produced after the chemical reaction between the rock specimens and the H_2SO_4 solution, which would float on the surface of CaO to prevent the sulfuric acid from contacting CaO, thus interfering in the chemical reaction. This interference explains the observation that, after 30 freeze-thaw cycles, the rock specimens in the H_2SO_4 solution were not seriously damaged, and only the rock surface demonstrated corrosion and peeling off (Figure 3). Therefore, there were relatively few sediments that could be observed during the experiment.

In addition, in the coupling environment of freeze-thaw and chemical effect, the red sandstones treated in H_2SO_4 solution were clearly affected by the freeze-thaw effect. When the temperature was low, the water or solution in the pores expanded due to freezing and produced pairs of frosting-heaving forces on the sidewalls of the mineral particles, causing the development and expansion of cracks within the rocks, and increase in porosity [38, 39]. When the temperature rose, the frozen water and chemical solution melted and moved into newly formed cracks, and the acid solution and the mineral elements within the rocks reacted with each other, so that part of the minerals were dissolved and separated and migrated out of the rocks. Therefore, cavities were formed in the rock specimens, causing the pores to develop and expand continuously. The number of mesopores and macropores increased, as displayed in Table 3, which enhanced the rock damaging process. With the progressive increase of freeze-thaw cycles, the cracks in the rock fabric kept developing and expanding, leading to the gradual increase of porosity. In the meantime, as the chemical solution from the outside entered the newly formed cracks and reacted with the mineral elements of the rocks, the cohesive force between the mineral particles was weakened periodically, which further accelerated the rock damage leading to macroscopic deterioration of the rock structures.

6. Conclusions

In summary, the coupling effects of acid solution and freeze-thaw had a significant influence on the microstructure of the

red sandstone rock specimens. The coupled effects are supported by observations that rock specimens immersed in the H_2SO_4 solution were damaged more adversely than rock specimens immersed in pure water. The differences in the preconditioned states of the two categories of specimens prior to exposure to freeze-thaw cycles account for the different types of pore structures observed, with significant implications for bulk permeability and macroscopic mechanical properties. The following conclusions can be made:

(1) Compared with the sandstone specimens in pure water, the freeze-thaw deterioration of the sandstone specimens is more severe under acidic conditions. The mass of the rock specimens decreases evidently with the increasing number of freeze-thaw cycles, and large particles peel off and fragments fall from the surface of the rock specimens.

(2) The H_2SO_4 solution has a large effect on the changes in porosity of the sandstone specimens. With the increasing number of freeze-thaw cycles, the trend in a linearly increasing porosity becomes clear, given that the acid environment has accelerated the development and expansion of the cracks within the specimens.

(3) As the number of freeze-thaw cycles increases, the pore structure of the rocks changes evidently under the acidic conditions. After 30 freeze-thaw cycles, the total spectral area of the rock specimen #C7 (in H_2SO_4 solution) increased by 35.6%, and the number of peaks increased from 4 to 6. In the meantime, the total spectral area of the rock specimen #F7 (in pure water) increased by 21%, and the number of peaks increased from 4 to 5. In addition, the trend of each spectra peak is also different.

(4) The MRI of the freeze-thaw deterioration of the sandstones under the acidic environment shows that the freeze-thaw deterioration of the sandstones is a gradual process which develops from the exterior to the interior and is much more severe than observed for the rock specimens in pure water. Therefore, the chemical environment will produce significant effects on the freeze-thaw deterioration of the rock specimens.

(5) Typically the pore sizes can be classified into four categories: micropores, minipores, mesopores, and macropores. After 30 freeze-thaw cycles, differences occur in the changes of the pore structure of sandstones in the H_2SO_4 solution and pure water: in H_2SO_4 solution, the numbers of mesopores and macropores grow, while the numbers of micropores and minipores decline. In contrast, in the pure water, micropores and macropores increase, while the minipores and mesopores decline.

(6) In the coupling environment of freeze-thaw and chemical effect, cracks within the red sandstone develop and expand continuously with the influence of the freeze-grow force, which causes the porosity to increase. Furthermore, as H_2SO_4 solution enters periodically into new cracks and react with mineral elements, part of the minerals are dissolved and separated out, which accelerates the rock damage process. However, given that the major compounds SiO_2 and H_2SO_4 in sandstone react slowly or do not react at all, the mass change of rock specimens is relatively small. Finally, the generation of the slightly soluble compound $CaSO_4$ affects the chemical reaction and slows down the deterioration of the interior structure of the rock specimens.

Data Availability

This study was supported by multiple datasets, which are openly available at locations cited in the reference section.

Conflicts of Interest

The authors declare that there are no conflicts of interest regarding the publication of this paper.

Acknowledgments

This work was supported by the National Natural Science Foundation of China (nos. 41502327, 51474252, and 51774323), National Major Scientific Instruments and Equipment Development Projects (2013YQ17046310), and Open-End Fund for the Valuable and Precision Instruments of Central South University (CSUZC201801). The first author would like to acknowledge the China Scholarship Council for financial support to the visiting scholar (201706375077) at the Colorado School of Mines.

References

[1] P. Li, J. Liu, G. H. Li, J. B. Zhu, and S. G. Liu, "Experimental study for shear strength characteristics of sandstone under water-rock interaction effects," *Rock and Soil Mechanics*, vol. 32, no. 2, pp. 380–386, 2011.

[2] W. X. Ding and X. T. Feng, "Damage effect and fracture criterion of rock with multi-preexisting cracks under chemical erosion," *Chinese Journal of Geotechnical Engineering*, vol. 31, no. 6, pp. 899–904, 2009.

[3] B. K. Atkinson and P. G. Meredith, "Stress corrosion cracking of quartz: a note on the influence of chemical environment," *Ectonophysics*, vol. 77, no. 1-2, pp. 1–11, 1981.

[4] P. Vazquez, L. Carrizo, C. Thomachot-Schneider, S. Gibeaux, and F. J. Alonso, "Influence of surface finish and composition on the deterioration of building stones exposed to acid atmospheres," *Construction and Building Materials*, vol. 106, pp. 392–403, 2016.

[5] L. J. Feucht and J. M. Logan, "Effects of chemically active solutions on shearing behavior of a sandstone," *Tectonophysics*, vol. 175, no. 1–3, pp. 159–176, 1990.

[6] S. L. Chen, X. T. Feng, and H. Zhou, "Study on triaxial mesofailure mechanism and damage variables of sandstone under chemical erosion," *Rock and Soil Mechanics*, vol. 25, no. 9, pp. 1363–1367, 2004.

[7] W. X. Ding and X. T. Feng, "CT experimental research of fractured rock failure process under chemical corrosion and permeation," *Chinese Journal of Rock Mechanics and Engineering*, vol. 27, no. 9, pp. 1865–1873, 2008.

[8] H. Y. Yao, X. T. Feng, Q. Cui et al., "Meso-mechanical experimental study of meso-fraeturing process of limestone under coupled chemical corrosion and water pressure," *Rock and Soil Mechanics*, vol. 30, no. 1, pp. 59–78, 2009.

[9] K.-B. Min, J. Rutqvist, and D. Elsworth, "Chemically and mechanically mediated influences on the transport and mechanical characteristics of rock fractures," *International Journal of Rock Mechanics and Mining Sciences*, vol. 46, no. 1, pp. 80–89, 2009.

[10] Y. S. Liu, W. Liu, and X. Y. Dong, "Dynamic mechanical properties and constitutive model of rock under chemical corrosion," *Journal of Yangtze River Scientific Research Institute*, vol. 32, no. 5, pp. 72–75, 2015.

[11] N. Li, Y. Zhu, B. Su, and S. Gunter, "A chemical damage model of sandstone in acid solution," *International Journal of Rock Mechanics and Mining Sciences*, vol. 40, no. 2, pp. 243–249, 2003.

[12] R. H. Brzesowsky, S. J. T. Hangx, N. Brantut, and C. J. Spiers, "Compaction creep of sands due to time-dependent grain failure: effects of chemical environment, applied stress, and grain size," *Journal of Geophysical Research Solid Earth*, vol. 119, no. 10, pp. 7521–7541, 2014.

[13] S. Miao, M. Cai, Q. Guo, P. Wang, and M. Liang, "Damage effects and mechanisms in granite treated with acidic chemical solutions," *International Journal of Rock Mechanics and Mining Sciences*, vol. 88, pp. 77–86, 2016.

[14] H. Zheng, X.-T. Feng, and P.-Z. Pan, "Experimental investigation of sandstone properties under CO_2–NaCl solution-rock interactions," *International Journal of Greenhouse Gas Control*, vol. 37, pp. 451–470, 2015.

[15] T. L. Han, Y. S. Chen, J. P. Shi et al., "Experimental study of mechanical characteristics of sandstone subjected to hydrochemical erosion," *Chinese Journal of Rock Mechanics and Engineering*, vol. 32, no. 13, pp. 146–159, 2013.

[16] J. L. Li, *Experiment study on deterioration mechanism of rock under the conditions of freezing-thawing cycles in cold regions based on NMR technology*, Ph.D. dissertation, Central South University, Changsha, China, 2012.

[17] W. G. Tian, *Experiment study on freezing-thawing damage mechanism of rock under the condition of Coupling of multiple factors*, Ph.D. dissertation, Central South University, Changsha, China, 2013.

[18] B. K. Ning, S. L. Chen, Q. Zhang et al., "Double corrosion effects under acid and freezing and thawing erosion and fracture behavior of concrete," *Journal of Shenyang University of Technology*, vol. 27, no. 5, pp. 575–578, 2005.

[19] X. Shi, L. Fay, M. M. Peterson, and Z. Yang, "Freeze-thaw damage and chemical change of a portland cement concrete in the presence of diluted deicers," *Materials and Structures*, vol. 43, no. 7, pp. 933–946, 2009.

[20] L. H. Lu, S. L. Chen, B. K. Ning et al., "Test study on concrete mechanical effect under together work of chemistry and frost and thaw torrosion," *Highway*, vol. 51, no. 8, pp. 154–158, 2006.

[21] F. Gao, Q. Wang, H. Deng, J. Zhang, W. Tian, and B. Ke, "Coupled effects of chemical environments and freeze-thaw cycles on damage characteristics of red sandstone," *Bulletin of Engineering Geology and the Environment*, vol. 76, no. 4, pp. 1481–1490, 2016.

[22] http://www.niumag.com/category/products.

[23] Suzhou Niumag Electronic Technology Co., Ltd., *NMR Rock-Core Analyzing Software Manual (Version 1.1.0)*, Suzhou Niumag Electronic Technology Co., Ltd., Suzhou, China, 2013, in Chinese.

[24] R. L. Kleinberg, "Utility of NMR T_2 distributions, connection with capillary pressure, clay effect, and determination of the surface relaxivity parameter rho 2," *Magnetic Resonance Imaging*, vol. 14, no. 7-8, pp. 761–767, 1996.

[25] X. M. Ge, Y. R. Fan, X. J. Zhu, Y. Chen, and R. Li, "Determination of nuclear magnetic resonance T_2 cutoff value based on multifractal theory—an application in sandstone with complex pore structure," *Geophysics*, vol. 80, no. 1, pp. 11–21, 2015.

[26] P. J. M. Monteiro, S. J. Bastacky, and T. L. Hayes, "Low-temperature scanning electron microscope analysis of the Portland cement paste early hydration," *Cement and Concrete Research*, vol. 15, no. 4, pp. 687–693, 1985.

[27] M. Hori and H. Morihiro, "Micromechanical analysis of deterioration due to freezing and thawing in porous brittle materials," *International Journal of Engineering Science*, vol. 36, no. 4, pp. 511–522, 1998.

[28] K. R. Brownstein and C. E. Tarr, "Importance of classical diffusion in NMR studies of water in biological cells," *Physical Review A*, vol. 19, no. 6, pp. 2446–2453, 1979.

[29] R. L. Kleinberg, W. E. Kenyon, and P. P. Mitra, "Mechanism of NMR relaxation of fluids in rock," *Journal of Magnetic Resonance*, vol. 108, no. 2, pp. 206–214, 1994.

[30] C. H. Lyu, Z. H. Ning, Q. Wang, and M. Chen, "Application of NMR T_2 to pore size distribution and movable fluid distribution in tight sandstones," *Energy Fuels*, vol. 32, no. 2, pp. 1395–1405, 2018.

[31] H. B. Li, J. Y. Zhu, and H. K. Guo, "Methods for calculating pore radius distribution in rock from NMR T_2 spectra," *Chinese Journal of Magnetic Resonance*, vol. 25, pp. 273–280, 2008.

[32] H. Zhou, F. Gao, X. Zhou et al., "The translation research of different types sandstone of Yungang Grottoes in NMR T_2-mercury capillary pressure," *Progress in Geophys*, vol. 28, no. 5, pp. 2759–2766, 2013.

[33] L. Z. Xiao, *Magnetic Resonance Imaging Well Logging and Rock Magnetic Resonance and Its Applications*, Science Press, Beijing, China, 1998.

[34] W. Z. Shao, J. Y. Xie, X. R. Chi et al., "On the relation of porosity and permeability in low porosity and low permeability rock," *Well Logging Technology*, vol. 37, no. 2, pp. 149–153, 2013.

[35] J. P. Yan, D. N. Wen, Z. Z. Li et al., "The quantitative evaluation method of low permeable sandstone pore structure based on nuclear magnetic resonance (NMR) logging: a case study of Es_4 formation in the south slope of dongying sag," *Chinese Journal of Geophysics*, vol. 59, no. 3, pp. 313–322, 2016.

[36] B. Gou, J. C. Guo, and T. Yu, "New method for calculating rock fracture pressure by acid damage," *Journal of Central South University (Science and Technology)*, vol. 46, no. 1, pp. 275–281, 2015.

[37] M. A. Mahmoud, H. A. Nasr-El-Din, C. A. DeWolf et al., "Sandstone acidizing using a new class of chelating agents," in *Proceedings of the SPE International Symposium on Oilfield Chemistry*, pp. 1–17, Society of Petroleum Engineers, The Woodlands, TX, USA, April 2011.

[38] I. C. McDowall, "Particle size reduction of clay minerals by freezing and thawing," *New Zealand Journal of Geology and Geophysics*, vol. 3, no. 3, pp. 337–343, 1960.

[39] T. Ishikawa and S. Miura, "Influence of freeze-thaw action on deformation-strength characteristics and particle crushability of volcanic coarse-grained soils," *Soils and Foundations*, vol. 51, no. 5, pp. 785–799, 2011.

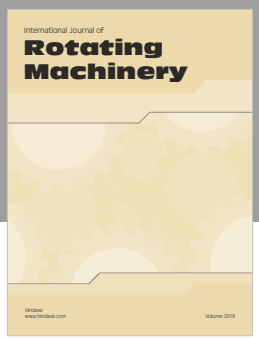

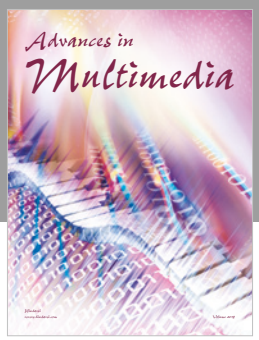

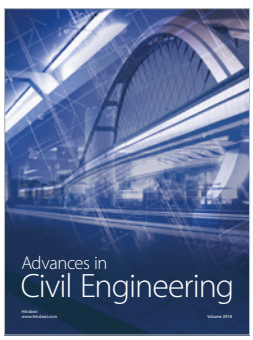

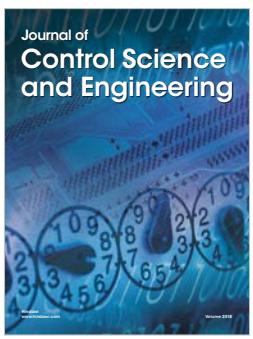

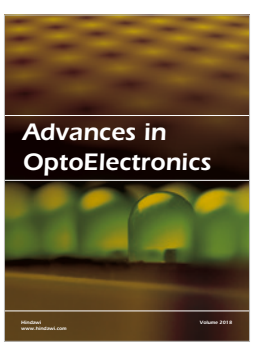

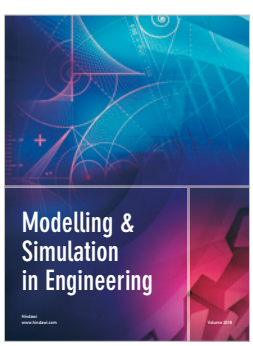

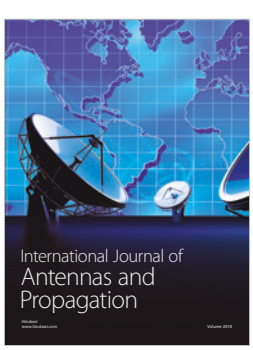

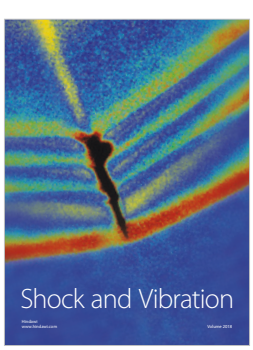

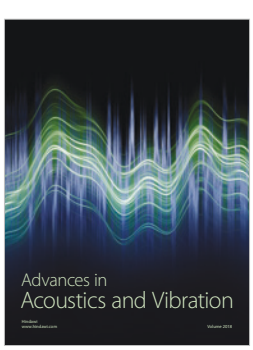

Hindawi

Submit your manuscripts at
www.hindawi.com